PHYSICAL REVIEW A **93**, 051402(R) (2016)

Possibility of introducing spin into attoscience with spin-polarized electrons produced by a bichromatic circularly polarized laser field

D. B. Milošević

Faculty of Science, University of Sarajevo, Zmaja od Bosne 35, 71000 Sarajevo, Bosnia and Herzegovina; Academy of Sciences and Arts of Bosnia and Herzegovina, Bistrik 7, 71000 Sarajevo, Bosnia and Herzegovina; and Max-Born-Institut, Max-Born-Strasse 2a, 12489 Berlin, Germany

(Received 5 January 2016; published 9 May 2016)

We show that the electrons, produced in strong-bicircular-field-induced above-threshold ionization of inert-gas atoms, have a large spin asymmetry if the ions exhibit fine-structure splitting. For a bicircular field, which consists of two coplanar counterrotating circularly polarized fields of frequencies ω and 2ω, the spin-asymmetry parameter changes rapidly with the electron energy. Since the electron–parent-ion rescattering in a counterrotating bicircular field is characterized on the attosecond time scale, this spin asymmetry may introduce the spin degree of freedom into attoscience. We show that the high-energy backward and low-energy forward scattered electrons, which are produced on the scale of a fraction of the laser cycle, exhibit spin asymmetry.

DOI: 10.1103/PhysRevA.93.051402

Since 1922 [1] the electron spin has attracted the attention of physicists. In the Stern-Gerlach experiment atoms were polarized and this method was not applicable to select polarization of free electrons. It took 50 years to find a method to obtain spin-polarized electrons by photoionization of polarized atoms (see Ch. 5.1 in [2]). Furthermore, Fano has shown in 1969 [3] that polarized electrons can be obtained by photoionization of nonpolarized atoms by circularly polarized light (Fano effect). In subsequent years this method was generalized to multiphoton ionization [4]. The main goal of the present Rapid Communication is to show that in above-threshold ionization of inert gases having the p ground state using a bicircular laser field which consists of two coplanar corotating or counterrotating circularly polarized fields having frequencies ω and 2ω it is possible to obtain polarized electrons whose spin varies rapidly with the change of the emitted electron momentum. The physical mechanism to produce polarized electrons suggested in this Rapid Communication is completely different than that of Ref. [4] and belongs to the realm of strong-field physics. Furthermore, we will show that the counterrotating bicircular field enables both spin asymmetry and rescattering of the ionized electron on the parent ion, which happens within a fraction of the laser-field cycle and is characterized by the attosecond dynamics.

Above-threshold ionization (ATI) is a process in which more photons are absorbed from an intense laser field than is necessary for ionization. The photoelectron energy spectrum consists of a series of peaks separated by photon energy ω. In the first observation of ATI of xenon atoms in 1979 [5] two such peaks separated by the photon energy of $\approx$2.4 eV were observed. In photoionization of Xe atoms there are two continua corresponding to two ground states of Xe^+ ion ($^2P_{3/2}$ and $^2P_{1/2}$) which have a fine-structure splitting of 1.31 eV. Three ATI peaks for each of these continua were observed in [6]. In the next decades there was a lot of new insights and discoveries connected with ATI (see, for example, review articles [7–9]), but attention was not devoted to the analysis of this splitting.

The differential ionization rate for ATI of atoms in initial state ψ_i by a $T = 2\pi/\omega$-periodic laser field with the electric field vector $\mathbf{E}(t)$, with emission of an electron having momentum $\mathbf{p}$ and energy $E_\mathbf{p} = \mathbf{p}^2/2$, and with absorption of n photons from the laser field, can be written as $w_{\mathbf{p}i}(n) = 2\pi p|T_{\mathbf{p}i}(n)|^2$, where the T-matrix element for the direct ATI in the length gauge and strong-field approximation is [10–12] (in atomic units)

$$T_{\mathbf{p}i}(n) = \int_0^T \frac{dt}{T} \langle \mathbf{p} + \mathbf{A}(t)|\mathbf{r}\cdot\mathbf{E}(t)|\psi_i\rangle e^{i[S_\mathbf{p}(t)+I_p t]}, \quad (1)$$

where $dS_\mathbf{k}(t)/dt = [\mathbf{k}+\mathbf{A}(t)]^2/2$, $\mathbf{A}(t) = -\int^t \mathbf{E}(t')dt'$, and $|\mathbf{k}\rangle$ is a plane-wave ket vector such that $\langle \mathbf{r}|\mathbf{k}\rangle = (2\pi)^{-3/2}\exp(i\mathbf{k}\cdot\mathbf{r})$. The number of absorbed photons satisfies the energy-conserving condition: $n\omega = E_\mathbf{p} + I_p + U_p$, where $U_p = \int_0^T \mathbf{A}^2(\tau)d\tau/(2T)$ is the ponderomotive energy, and I_p is the ionization potential. This one-dimensional integral over the ionization time t can be calculated numerically or approximately solved using the saddle-point (SP) method.

We apply the SP method to ATI of inert atomic gases. In length gauge the interaction $\mathbf{r}\cdot\mathbf{E}(t)$ emphasizes large distances where the bound-state wave functions have well-defined asymptotic behavior, so that we can approximate these functions (in the spherical coordinates, with the z axis as axis of quantization) with [10]

$$\psi_{ilm}(\mathbf{r}) = \langle r\theta\phi|\psi_{ilm}\rangle = Ar^{\nu-1}\exp(-\kappa r)Y_{lm}(\theta,\phi), \quad (2)$$

where $Y_{lm}(\theta,\phi) = \langle\theta\phi|lm\rangle$ are normalized spherical harmonics in complex form, the constant A is tabulated in [13–15], $\nu = Z/\kappa$ ($Z = 1$ for atoms), and $\kappa = \sqrt{2I_p}$. The SP equation is determined by the condition $d[S_\mathbf{p}(t) + I_p t]/dt = 0$ which gives the energy-conserving condition at the ionization time t,

$$\tfrac{1}{2}[\mathbf{p} + \mathbf{A}(t)]^2 = -I_p. \quad (3)$$

After a partial integration over the time t in Eq. (1) the matrix element $\langle\mathbf{q}|\mathbf{r}\cdot\mathbf{E}(t)|\psi_i\rangle$, with $\mathbf{q} = \mathbf{p} + \mathbf{A}(t)$, is replaced by the function $-(I_p + \mathbf{q}^2/2)\tilde{\psi}_i(\mathbf{q})$, where $\tilde{\psi}_i(\mathbf{q}) = (2\pi)^{-3/2}\int d\mathbf{r}\,\psi_i(\mathbf{r})\exp(-i\mathbf{q}\cdot\mathbf{r})$ is the momentum space asymptotic wave function which can be expressed as a product of the Gauss hypergeometric series ${}_2F_1(a,b;c;-\mathbf{q}^2/\kappa^2)$ and the solid harmonics $Y_{lm}(\hat{\mathbf{q}})(q/\kappa)^l$. The SP equation implies

that $\mathbf{q}^2 = -\kappa^2$, so that, with a proper choice of the integration contour in the complex plane, one obtains [8,10,16]

$$T_{\mathbf{p}i}^{\mathrm{SP}}(n) = i2^{-3/2}T^{-1}A\kappa^{\nu}\nu\Gamma(\nu/2) \times \sum_s \left(\frac{q_s}{i\kappa}\right)^l Y_{lm}(\hat{\mathbf{q}}_s)\left(\frac{2i}{S_s''}\right)^{(\nu+1)/2} e^{iS_s}, \quad (4)$$

where $\mathbf{q}_s = \mathbf{p} + \mathbf{A}(t_s)$, $S_s = S_{\mathbf{p}}(t_s) + I_p t_s$, and $S_s'' = -\mathbf{E}(t_s)\cdot[\mathbf{p} + \mathbf{A}(t_s)]$. The summation in Eq. (4) is over those complex SP solutions of Eq. (3) for the ionization time t that are in the upper half of the complex t plane. Our bicircular field is defined in the xy plane with

$$E_x(t) = [E_1\sin(\omega t) + E_2\sin(2\omega t)]/\sqrt{2},$$
$$E_y(t) = [-E_1\cos(\omega t) \mp E_2\cos(2\omega t)]/\sqrt{2}, \quad (5)$$

where in the second term in the second row the sign is "−" ("+") for corotating (counterrotating) components. For the bicircular field with corotating (counterrotating) components there are two (three) SP solutions [17].

We can expand wave functions which appear in our matrix element in any basis. For angular basis functions we used simultaneous eigenstates of the orbital angular momentum operators $\mathbf{L}^2$ and L_z, the spherical harmonics $\langle\theta\varphi|lm\rangle = Y_{lm}(\theta,\varphi)$. We can extend our basis vectors into the direct product $|lm\rangle|m_s\rangle$, where $|m_s\rangle$ are simultaneous eigenvectors of the spin operators $\mathbf{S}^2$ and S_z (the electron spin is $s = 1/2$ and $m_s = \pm 1/2$). The spin-orbit interaction gives an additional term in the Hamiltonian which contains the spin-orbit coupling operator $\mathbf{L}\cdot\mathbf{S} = (\mathbf{J}^2 - \mathbf{L}^2 - \mathbf{S}^2)/2$ [18], where $\mathbf{J} = \mathbf{L} + \mathbf{S}$ is the total angular momentum operator. Then, instead of the basis vectors $|lm\rangle|m_s\rangle$ we have to introduce new basis vectors which are simultaneous eigenvectors of the operators $\mathbf{J}^2$, J_z, $\mathbf{L}^2$, and $\mathbf{S}^2$. In our case we have the addition of orbital angular momentum and spin 1/2. For a given value of l two values of j are possible: $j = l \pm 1/2$, and the new basis vectors are given by

$$\left|l \pm \tfrac{1}{2}, m_j, l\right\rangle = \pm c_{lm_j}^{(\pm)}\left|l, m_j - \tfrac{1}{2}\right\rangle\left|m_s = \tfrac{1}{2}\right\rangle + c_{lm_j}^{(\mp)}\left|l, m_j + \tfrac{1}{2}\right\rangle\left|m_s = -\tfrac{1}{2}\right\rangle, \quad (6)$$

with $m_j = m + m_s$ and $c_{lm_j}^{(\pm)2} = (l \pm m_j + \frac{1}{2})/(2l+1)$.

We are using the single-active-electron approximation. However, different electrons from the ground state configuration of an atom can play the role of this active electron. The corresponding summed ionization rate can be calculated in any of the above-introduced bases, i.e.

$$W_{\mathbf{p}il} = W_{\mathbf{p}\uparrow} + W_{\mathbf{p}\downarrow} = \sum_{m_s=\pm 1/2}\sum_{m=-l,\ldots,l} w_{\mathbf{p}il}^{(m,m_s)} = \sum_{j=l\pm 1/2}\sum_{m_j=-j,\ldots,j} w_{\mathbf{p}il}^{[j,m_j]}\left(I_p^j\right), \quad (7)$$

where $W_{\mathbf{p}\uparrow}$ ($W_{\mathbf{p}\downarrow}$) denotes the rate for electrons having spin up (down), i.e., having $m_s = 1/2$ ($m_s = -1/2$). The rates in different bases are denoted by the upper indices in different bracketing: "$(\cdots)$" vs "$[\cdots]$." The basis $[j,m_j]$ includes spin-orbit coupling so that we added the dependence on the ionization potential I_p^j. In the case of Xe (as well as Kr) we have $I_p^{3/2} = I_p(^2P_{3/2})$ and $I_p^{1/2} = I_p(^2P_{1/2})$. Furthermore, for the laser electric field vector in the xy plane, it can be shown that only the T-matrix elements with $m = \pm 1$ are different from zero, so that, using Eq. (6) we can write

$$W_{\mathbf{p}\uparrow} = \tfrac{2}{3}w_{\mathbf{p}il}^{(-1,1/2)}\left(I_p^{1/2}\right) + \tfrac{1}{3}w_{\mathbf{p}il}^{(-1,1/2)}\left(I_p^{3/2}\right) + w_{\mathbf{p}il}^{(1,1/2)}\left(I_p^{3/2}\right), \quad (8)$$

$$W_{\mathbf{p}\downarrow} = \tfrac{2}{3}w_{\mathbf{p}il}^{(1,-1/2)}\left(I_p^{1/2}\right) + \tfrac{1}{3}w_{\mathbf{p}il}^{(1,-1/2)}\left(I_p^{3/2}\right) + w_{\mathbf{p}il}^{(-1,-1/2)}\left(I_p^{3/2}\right). \quad (9)$$

The asymmetry parameter $A_{\mathbf{p}} = (W_{\mathbf{p}\uparrow} - W_{\mathbf{p}\downarrow})/(W_{\mathbf{p}\uparrow} + W_{\mathbf{p}\downarrow})$ can easily be found by calculating the rates $w_{\mathbf{p}il}^{(m,m_s)} = 2\pi p|T_{\mathbf{p}i}(n)|^2$ using Eqs. (1)–(4) for $m = \pm 1$ and for the corresponding values of I_p, having in mind that the rate does not depend on m_s. For presentation in the momentum plane we will use the normalized asymmetry parameter, defined with respect to the maximal summed rate by the relation

$$\tilde{A}_{\mathbf{p}} = (W_{\mathbf{p}\uparrow} - W_{\mathbf{p}\downarrow})/\max_{\mathbf{p}}(W_{\mathbf{p}\uparrow} + W_{\mathbf{p}\downarrow}). \quad (10)$$

If we neglect the spin-orbit coupling, then $I_p^{1/2} = I_p^{3/2}$ and $A_{\mathbf{p}} = 0$. The asymmetry $A_{\mathbf{p}}$ is also zero if the rates are the same for $m = +1$ and $m = -1$. Therefore, in order to achieve a large asymmetry, i.e., to obtain a $\mathbf{p}$-dependent distribution of the polarized electrons, the spin-orbit coupling should be strong enough and the ground state and the laser field should be such that the rate shows strong $m = \pm 1$ asymmetry. This is the case for ATI of inert gases having p ground state by circularly polarized laser field [19,20] and for ionization by bicircular field [21,22]. The spin-polarized electrons produced by ionization of Kr atoms by a strong circularly polarized field were considered in [20]. It is important to notice that the spin polarization proposed in [20] does not open up access to attosecond spin effects, owing to the absence of rescattering for one circularly polarized field.

We present our numerical results for ATI of Xe atoms by bicircular ω-2ω laser field with equal intensities of both components $I_1 = E_1^2 = I_2 = E_2^2 = 1\times 10^{14}$ W/cm^2 and the fundamental wavelength of 800 nm. The ionization energies are $I_p^{3/2} = 12.14$ eV and $I_p^{1/2} = 13.44$ eV. For the corotating bicircular field components the photoelectron momentum distribution has a single crescent-shaped lobe [23,24] whose position depends on the value m. This m dependence (in addition to the I_p dependence), causes a large asymmetry parameter, which goes from $A_{\mathbf{p}} = -0.8815$ to 0.9384. However, the value of the normalized asymmetry parameter $\tilde{A}_{\mathbf{p}}$ (with respect to the maximal rate 2.7149×10^{-4} a.u.), shown in Fig. 1, is much smaller and has a crescentlike shape similar to that of the rates.

Next, we present the results for ATI by bicircular field having counterrotating components (the corresponding electric field vector and the vector potential are shown in the upper right panel in Fig. 3 below). In addition to the asymmetry parameter $\tilde{A}_{\mathbf{p}}$, in Fig. 2 we present the rates for $m = \pm 1$ (upper panels) and the rate summed over m (lower left panel). All presented results exhibit the symmetry with respect to the rotation by the angle 120° around the z axis [17]. In addition to this, one can notice the reflection symmetry with respect to the axes which

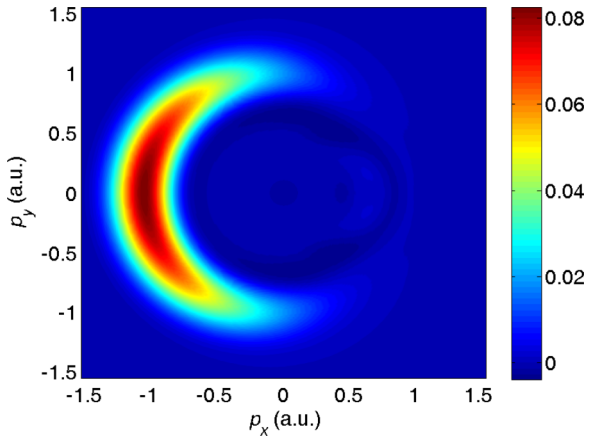

FIG. 1. Normalized asymmetry parameter $\tilde{A}_{\mathbf{p}}$, Eq. (10), presented in false colors in the electron momentum plane for ATI of Xe atoms by a bicircular ω-2ω laser field with equal intensities of both corotating components $I_1 = I_2 = 1 \times 10^{14}$ W/cm^2 and the fundamental wavelength of 800 nm.

are at the angles $\theta = 60^\circ$, 180°, and 300° with respect to the x axis [25]. Near these reflection axes the rates exhibit maxima which are at different positions for $m = \pm 1$. The asymmetry parameter $A_{\mathbf{p}}$ shows similar structure and oscillates between -0.4711 and 0.9347. The asymmetry parameter, normalized to the maximal rate 1.4892×10^{-4} a.u., shown in the lower right panel of Fig. 2, is stronger than that for the corotating case and can take the values $|\tilde{A}_{\mathbf{p}}| > 0.2$. The overall effect is that for a fixed electron emission angle, say 60°, the spin of the emitted electron considerably changes with the electron energy, and the corresponding asymmetry changes from a large positive to a large negative value.

In order to understand the rapidly changing structures which appear in the case of the counterrotating bicircular field, in Fig. 3 we present the field (upper right panel), the asymmetry parameter, the SP solutions, and the relevant quantum orbits, for the fixed electron emission angle $\theta = 60^\circ$ with respect to the x axis. From the lower right panel we see that $A_{\mathbf{p}}$ oscillates as a function of the electron energy between large negative and positive values. In the upper middle panel the ionization time is presented in the complex t plane. There are three SP solutions and the electron energy for each solution changes continuously from $0.02U_p$ to $5U_p$. The energy $E_{\mathbf{p}} = 2U_p$ is denoted by a square on each curve. The dominant contributions to the rate come from the two solutions that are symmetric with respect to $\mathrm{Re}\, t = 2T/3$. These contributions (red and green lines) interfere leading to the oscillatory structure of the rates and the

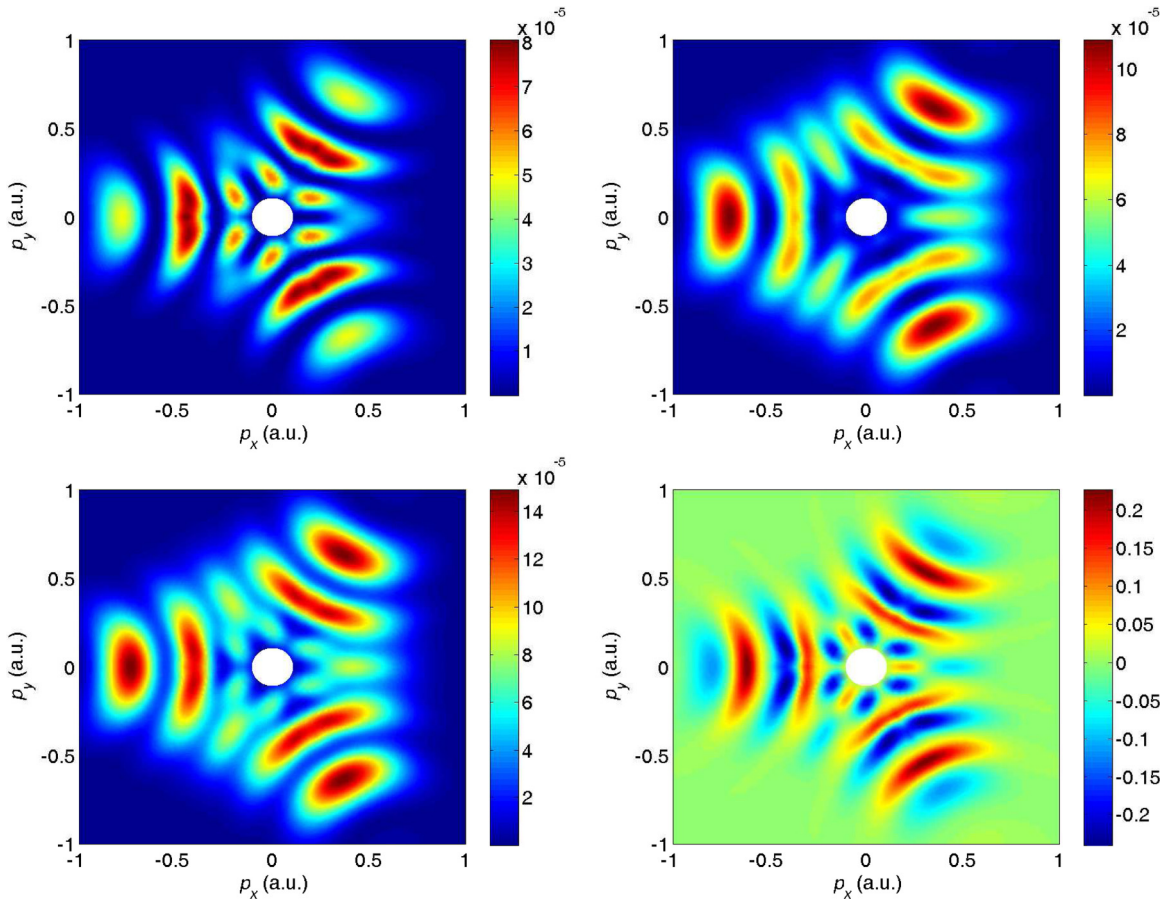

FIG. 2. The differential ionization rate (in a.u.) of Xe atoms, presented in false colors in the electron momentum plane for ionization by a bicircular ω-2ω laser field with equal intensity of both counterrotating components $I_1 = I_2 = 1 \times 10^{14}$ W/cm^2 and the fundamental wavelength of 800 nm. Upper panels: the rates for the initial states having the magnetic quantum number $m = -1$ (left) and $m = +1$ (right). Lower left panel: the rate summed over m. Lower right panel: normalized asymmetry parameter $\tilde{A}_{\mathbf{p}}$, Eq. (10).

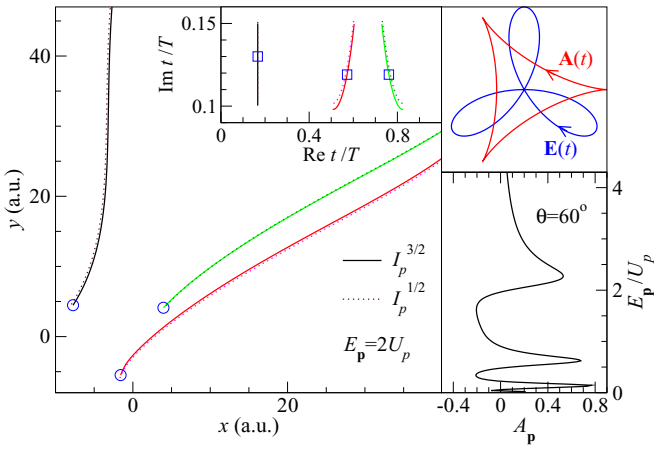

FIG. 3. Upper right panel: Bicircular electric field vector $\mathbf{E}(t)$ and the vector potential $\mathbf{A}(t)$ for $0 \leqslant t \leqslant T$. The electric field vector starts from the point $\mathbf{E}(0) = (0,0)$ and develops in the clockwise direction for $t > 0$, while the vector potential develops in a counterclockwise sense, as indicated by arrows. Lower right panel: Spin-asymmetry parameter $A_\mathbf{p}$ presented as a function of the electron energy $E_\mathbf{p}$ (in units of the ponderomotive energy U_p). Upper middle panel: Three complex SP solutions for the ionization time t (in units of the optical period T; the electron energy on each curve changes continuously from $0.02U_p$ to $5U_p$). Left panel: Electron trajectories for the SP solutions from the upper middle panel and fixed electron energy $E_\mathbf{p} = 2U_p$ (denoted by squares). The laser and atomic parameters are as in Fig. 2 and the electron emission angle is $\theta = 60^\circ$. Solid (dotted) lines correspond to the ionization potential $I_p^{3/2}$ ($I_p^{1/2}$).

asymmetry parameter. This situation is similar to the linearly polarized field case for $\theta = 0^\circ$ where also contributions of two solutions interfere [26]. For this energy we calculated quantum orbits and have shown the corresponding electron trajectories depicted by the curves having the same color as the curves for the SP solutions in the upper panel. Quantum orbits [7,8,27,28] are defined as solutions of the classical Newton's equation for the electron in the presence of the laser field, $\ddot{\mathbf{r}}(t) = -\mathbf{E}(t)$, for the complex ionization time t, while the electron trajectories are defined as the real part of $\mathbf{r}(t)$ for $\tau > \mathrm{Re}\, t$: $\mathbf{r}(\tau) = (\tau - t)\mathbf{p} + \int_t^\tau dt'\, \mathbf{A}(t')$. Since $\mathrm{Re}\, \mathbf{r}(\mathrm{Re}\, t) \neq \mathbf{0}$, the electron starts a few atomic units away from the origin (starting point, i.e., the exit of the tunnel, is denoted by a circle) and is driven by the laser field to the detector under the angle $\theta = 60^\circ$. Since the difference between the ionization potentials $I_p^{3/2}$ and $I_p^{1/2}$ is small, the difference between the corresponding trajectories, presented by solid and dotted lines, respectively, is also small. To summarize, the origin of the pronounced energy dependence of the spin asymmetry is in the interference of two dominant quantum-orbit contributions to the ionization rate. For a counterrotating bicircular field and a p ground state, this mechanism goes hand in hand with spin polarization.

For the counterrotating bicircular field the electron rescattering off the parent ion is important [25]. Using the improved strong-field approximation and quantum-orbit theory [25] it is possible to calculate the spin-asymmetry parameter which corresponds to the rescattering quantum orbits. In this case the asymmetry also obeys the threefold symmetry but we present in Fig. 4 only the results for $p_x > 0$ and $p_y > 0$. The

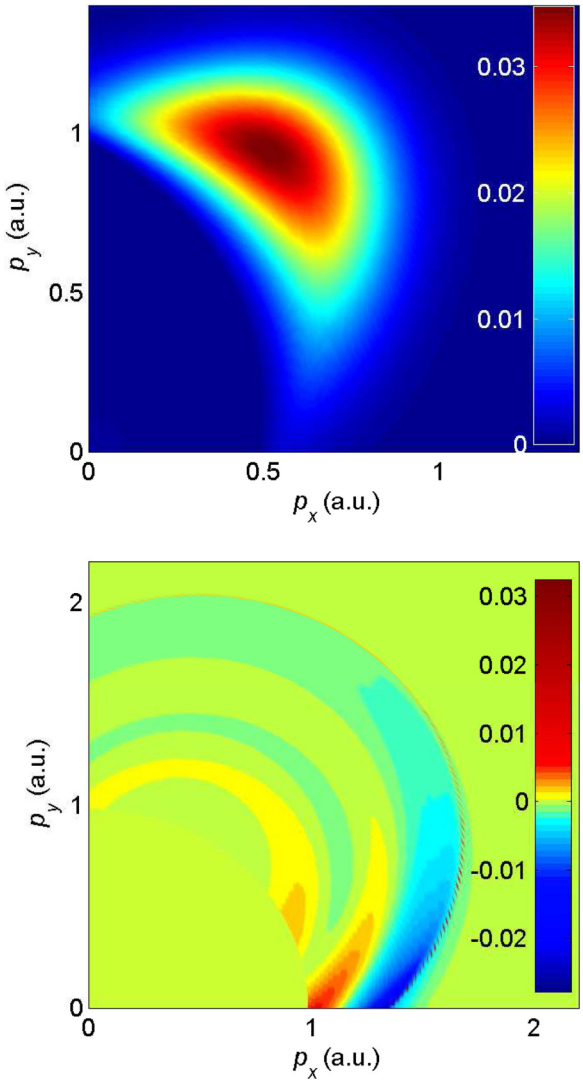

FIG. 4. Normalized asymmetry parameter $\tilde{A}_\mathbf{p}$ presented in false colors in the electron momentum plane for the same parameters as in Fig. 2. Results presented in the upper (lower) panel are obtained using the improved strong-field approximation and the shortest forward- (backward-) scattering quantum orbits.

most important is the contribution of the forward scattering, which is in accordance with the experimental results [23]. In the upper panel of Fig. 4 a pronounced maximum near $(p_x, p_y) = (0.6\text{ a.u.}, 1\text{ a.u.})$ is clearly visible. It appears exactly for the momentum for which the electrons were observed in the experiment [23]. These results in [23] were explained, using the solutions of the time-dependent Schrödinger equation, as a consequence of the Coulomb-field-enhanced forward scattering. In the lower panel of Fig. 4 we present the asymmetry parameter for the pair of the shortest backward-scattering quantum orbits. The interference of the contributions of these orbits is responsible for the momentum-dependent variation of the normalized asymmetry parameter. Since the backscattering electron energy can be large (recall the $10U_p$ cutoff law) the asymmetry appears for larger momenta ($\sim$2 a.u.) than in the previous figures. The spin asymmetry is the strongest for the angle $\theta = 0^\circ$ (and for the angles 120° and 240°, owing to the threefold symmetry).

Let us comment on why this momentum-dependent spin asymmetry is an important effect which can have various applications. It is known that for attoscience [29] the rescattering of the ionized electron on the parent ion is important [30]. This rescattering happens on a time scale which is a small part of the optical cycle (a few femtoseconds for usually used laser wavelengths). Therefore, recollisions happen on the attosecond time scale. For circular and corotating bicircular fields rescattering is not important. However, for a counterrotating bicircular field the electron (having a suitable nonzero initial momentum) can return to the parent ion and recombine emitting a high harmonic with high efficiency [31] (see also [32]). This process was explained using quantum-orbit theory and the relevant trajectories were identified [33]. More recently, this process has attracted great attention due to the possibility of emission of circularly polarized high harmonics [34–38]. In the present Rapid Communication we have shown that the spin of the emitted photoelectrons in ATI of Xe by counterrotating bicircular field strongly depends on the electron energy. One can expect interesting effects in the spin-dependent rescattering process which should appear in such field. The physics of polarized electron scattering is well established [39] and still vivid [40]. This can affect laser-induced electron diffraction [41], while in nonsequential double ionization [42] the role of the spin-dependent ionizing collision can be important. The polarized electrons obtained using our method can have many practical applications (for example, to study chiral molecules [43], magnetic materials [44], etc.). Having also in mind how the electron spin is important for spintronics [45] (see also Chap. 2 in [46]) we expect that the introduction of the electron spin into the strong-field physics may represent a milestone for this field.

We gratefully acknowledge useful discussion with Wilhelm Becker.

[1] W. Gerlach and O. Stern, Der experimentelle Nachweis der Richtungsquantelung im Magnetfeld, Z. Phys. **9**, 349 (1922); Das magnetische Moment des Silberatoms, *ibid.* **9**, 353 (1922).

[2] J. Kessler, *Polarized Electrons*, 2nd ed. (Springer-Verlag, Berlin, 1985).

[3] U. Fano, Spin orientation of photoelectrons ejected by circularly polarized light, Phys. Rev. **178**, 131 (1969); Spin orientation of photoelectrons: Erratum and addendum, *ibid.* **184**, 250 (1969).

[4] P. Lambropoulos, Topics on multiphoton processes in atoms, Adv. At. Mol. Phys. **12**, 87 (1976); S. N. Dixit, P. Lambropoulos, and P. Zoller, Spin polarization of electrons in two-photon resonant three-photon ionization, Phys. Rev. A **24**, 318 (1981); T. Nakajima and P. Lambropoulos, Electron spin-polarization in single-, two- and three-photon ionization of xenon, Europhys. Lett. **57**, 25 (2002).

[5] P. Agostini, F. Fabre, G. Mainfray, G. Petite, and N. K. Rahman, Free-Free Transitions Following Six-Photon Ionization of Xenon Atoms, Phys. Rev. Lett. **42**, 1127 (1979).

[6] F. Fabre, G. Petite, P. Agostini, and M. Clement, Multiphoton above-threshold ionisation of xenon at 0.53 and 1.06 μm, J. Phys. B **15**, 1353 (1982).

[7] W. Becker, F. Grasbon, R. Kopold, D. B. Milošević, G. G. Paulus, and H. Walther, Above-threshold ionization: From classical features to quantum effects, Adv. At., Mol., Opt. Phys. **48**, 35 (2002).

[8] D. B. Milošević, G. G. Paulus, D. Bauer, and W. Becker, Above-threshold ionization by few-cycle pulses, J. Phys. B **39**, R203 (2006).

[9] P. Agostini and L. F. DiMauro, Atomic and molecular ionization dynamics in strong laser fields: From optical to X-rays, Adv. At., Mol., Opt. Phys. **61**, 117 (2012).

[10] G. F. Gribakin and M. Yu. Kuchiev, Multiphoton detachment of electrons from negative ions, Phys. Rev. A **55**, 3760 (1997).

[11] D. B. Milošević and F. Ehlotzky, Coulomb corrections in above-threshold ionization in a bichromatic laser field, J. Phys. B **31**, 4149 (1998); Coulomb and rescattering effects in above-threshold ionization, Phys. Rev. A **58**, 3124 (1998); S-matrix theory of above-threshold ionization in a bichromatic laser field, J. Phys. B **32**, 1585 (1999).

[12] D. B. Milošević, A. Gazibegović-Busuladžić, and W. Becker, Direct and rescattered electrons in above-threshold detachment from negative ions, Phys. Rev. A **68**, 050702(R) (2003); A. Gazibegović-Busuladžić, D. B. Milošević, and W. Becker, High-energy above-threshold detachment from negative ions, *ibid.* **70**, 053403 (2004).

[13] A. A. Radzig and B. M. Smirnov, *Reference Data on Atoms, Molecules and Ions* (Springer, Berlin, 1985).

[14] X. M. Tong, Z. X. Zhao, and C. D. Lin, Theory of molecular tunneling ionization, Phys. Rev. A **66**, 033402 (2002).

[15] T. K. Kjeldsen and L. B. Madsen, Strong-field ionization of diatomic molecules and companion atoms: Strong-field approximation and tunneling theory including nuclear motion, Phys. Rev. A **71**, 023411 (2005).

[16] T. K. Kjeldsen and L. B. Madsen, Strong-field ionization of atoms and molecules: The two-term saddle-point method, Phys. Rev. A **74**, 023407 (2006).

[17] A. Kramo, E. Hasović, D. B. Milošević, and W. Becker, Above-threshold detachment by a two-color bicircular laser field, Laser Phys. Lett. **4**, 279 (2007); E. Hasović, A. Kramo, and D. B. Milošević, Energy- and angle-resolved photoelectron spectra of above-threshold ionization and detachment, Eur. Phys. J.: Spec. Top. **160**, 205 (2008).

[18] H. Friedrich, *Theoretical Atomic Physics* (Springer-Verlag, Berlin, 1991).

[19] T. Herath, L. Yan, S. K. Lee, and W. Li, Strong-Field Ionization Rate Depends on the Sign of the Magnetic Quantum Number, Phys. Rev. Lett. **109**, 043004 (2012).

[20] I. Barth and O. Smirnova, Spin-polarized electrons produced by strong-field ionization, Phys. Rev. A **88**, 013401 (2013); Comparison of theory and experiment for nonadiabatic tunneling in circularly polarized fields, *ibid.* **87**, 065401 (2013).

[21] D. B. Milošević, Generation of elliptically polarized attosecond pulse trains, Opt. Lett. **40**, 2381 (2015); Circularly polarized high harmonics generated by a bicircular field from inert atomic

gases in the p state: A tool for exploring chirality-sensitive processes, Phys. Rev. A **92**, 043827 (2015).

[22] L. Medišauskas, J. Wragg, H. van der Hart, and M. Yu. Ivanov, Generating Isolated Elliptically Polarized Attosecond Pulses using Bichromatic Counterrotating Circularly Polarized Laser Fields, Phys. Rev. Lett. **115**, 153001 (2015).

[23] C. A. Mancuso, D. D. Hickstein, P. Grychtol, R. Knut, O. Kfir, X. M. Tong, F. Dollar, D. Zusin, M. Gopalakrishnan, C. Gentry, E. Turgut, J. L. Ellis, M.-C. Chen, A. Fleischer, O. Cohen, H. C. Kapteyn, and M. M. Murnane, Strong-field ionization with two-color circularly polarized laser fields, Phys. Rev. A **91**, 031402(R) (2015).

[24] C. A. Mancuso, D. D. Hickstein, K. M. Dorney, J. L. Ellis, E. Hasović, R. Knut, P. Grychtol, C. Gentry, M. Gopalakrishnan, D. Zusin, F. J. Dollar, X.-M. Tong, D. B. Milošević, W. Becker, H. C. Kapteyn, and M. M. Murnane, Controlling electron-ion rescattering in two-color circularly polarized femtosecond laser fields, Phys. Rev. A **93**, 053406 (2016).

[25] E. Hasović, W. Becker, and D. B. Milošević, Electron rescattering in a bicircular laser field, Opt. Express **24**, 6413 (2016).

[26] Ph. A. Korneev, S. V. Popruzhenko, S. P. Goreslavski, W. Becker, G. G. Paulus, B. Fetić, and D. B. Milošević, Interference structure of above-threshold ionization versus above-threshold detachment, New J. Phys. **14**, 055019 (2012); For linear polarization the spin-asymmetry parameter is zero. Bicircular counterrotating field provides both the rescattering, which is characteristic for linear polarization, and the spin asymmetry, which appears for circular polarization.

[27] P. Salières, B. Carré, L. Le Déroff, F. Grasbon, G. G. Paulus, H. Walther, R. Kopold, W. Becker, D. B. Milošević, A. Sanpera, and M. Lewenstein, Feynman's path-integral approach for intense-laser–atom interactions, Science **292**, 902 (2001).

[28] D. B. Milošević, D. Bauer, and W. Becker, Quantum-orbit theory of high-order atomic processes in intense laser fields, J. Mod. Opt. **53**, 125 (2006).

[29] F. Krausz and M. Ivanov, Attosecond physics, Rev. Mod. Phys. **81**, 163 (2009).

[30] P. B. Corkum, Plasma Perspective on Strong Field Multiphoton Ionization, Phys. Rev. Lett. **71**, 1994 (1993).

[31] H. Eichmann, A. Egbert, S. Nolte, C. Momma, B. Wellegehausen, W. Becker, S. Long, and J. K. McIver, Polarization-dependent high-order two-color mixing, Phys. Rev. A **51**, R3414(R) (1995); S. Long, W. Becker, and J. K. McIver, Model calculations of polarization-dependent two-color high-harmonic generation, *ibid.* **52**, 2262 (1995).

[32] T. Zuo and A. D. Bandrauk, High-order harmonic generation in intense laser and magnetic fields, J. Nonlinear Opt. Phys. Mater. **04**, 533 (1995).

[33] D. B. Milošević, W. Becker, and R. Kopold, Generation of circularly polarized high-order harmonics by two-color coplanar field mixing, Phys. Rev. A **61**, 063403 (2000); D. B. Milošević and W. Sandner, Extreme-ultraviolet harmonic generation near 13 nm with a two-color elliptically polarized laser field, Opt. Lett. **25**, 1532 (2000); D. B. Milošević, W. Becker, R. Kopold, and W. Sandner, High-harmonic generation by a bichromatic bicircular laser field, Laser Phys. **11**, 165 (2001).

[34] D. B. Milošević and W. Becker, Attosecond pulse trains with unusual nonlinear polarization, Phys. Rev. A **62**, 011403(R) (2000); Attosecond pulse generation by bicircular fields: From pulse trains to a single pulse, J. Mod. Opt. **52**, 233 (2005).

[35] A. Fleischer, O. Kfir, T. Diskin, P. Sidorenko, and O. Cohen, Spin angular momentum and tunable polarization in high-harmonic generation, Nat. Photonics **8**, 543 (2014).

[36] O. Kfir, P. Grychtol, E. Turgut, R. Knut, D. Zusin, D. Popmintchev, T. Popmintchev, H. Nembach, J. M. Shaw, A. Fleischer, H. Kapteyn, M. Murnane, and O. Cohen, Generation of bright phase-matched circularly-polarized extreme ultraviolet high harmonics, Nat. Photonics **9**, 99 (2015).

[37] T. Fan *et al.*, Bright circularly polarized soft X-ray high harmonics for X-ray magnetic circular dichroism, Proc. Natl. Acad. Sci. U.S.A. **112**, 14206 (2015).

[38] C. Chen, Z. Tao, C. Hernández-García, P. Matyba, A. Carr, R. Knut, O. Kfir, D. Zusin, C. Gentry, P. Grychtol, O. Cohen, L. Plaja, A. Becker, A. Jaron-Becker, H. Kapteyn, and M. Murnane, Tomographic reconstruction of circularly polarized high-harmonic fields: 3D attosecond metrology, Sci. Adv. **2**, e1501333 (2016).

[39] G. F. Drukarev, *Collisions of Electrons with Atoms and Molecules* (Plenum, New York, 1997).

[40] T. J. Gay, Physics and technology of polarized electron scattering from atoms and molecules, Adv. At., Mol., Opt. Phys. **57**, 157 (2009).

[41] M. Meckel, D. Comtois, D. Zeidler, A. Staudte, D. Pavičić, H. C. Bandulet, H. Pépin, J. C. Kieffer, R. Dörner, D. M. Villeneuve, and P. B. Corkum, Laser-induced electron tunneling and diffraction, Science **320**, 1478 (2008); C. I. Blaga, J. Xu, A. D. DiChiara, E. Sistrunk, K. Zhang, P. Agostini, T. A. Miller, L. F. DiMauro, and C. D. Lin, Imaging ultrafast molecular dynamics with laser-induced electron diffraction, Nature (London) **483**, 194 (2012).

[42] W. Becker, X. Liu, P. J. Ho, and J. H. Eberly, Theories of photoelectron correlation in laser-driven multiple atomic ionization, Rev. Mod. Phys. **84**, 1011 (2012).

[43] N. Böwering, T. Lischke, B. Schmidtke, N. Müller, T. Khalil, and U. Heinzmann, Asymmetry in Photoelectron Emission from Chiral Molecules Induced by Circularly Polarized Light, Phys. Rev. Lett. **86**, 1187 (2001); M. H. M. Janssen and I. Powis, Detecting chirality in molecules by imaging photoelectron circular dichroism, Phys. Chem. Chem. Phys. **16**, 856 (2014).

[44] J. Stöhr, Y. Wu, B. D. Hermsmeier, M. G. Samant, G. R. Harp, S. Koranda, D. Dunham, and B. P. Tonner, Element-specific magnetic microscopy with circularly polarized X-rays, Science **259**, 658 (1993).

[45] I. Žutić, J. Fabian, and S. Das Sarma, Spintronics: Fundamentals and applications, Rev. Mod. Phys. **76**, 323 (2004).

[46] *Magnetism and Synchrotron Radiation: New Trends*, edited by E. Beaurepaire, H. Bulou, F. Scheurer, and J. P. Kappler (Springer, Heidelberg, 2010).